Requirement of cellular DDX3 for hepatitis C virus replication is unrelated to its interaction with the viral core protein

Allan G. N. Angus,[1] David Dalrymple,[1] Steeve Boulant,[1] David R. McGivern,[2] Reginald F. Clayton,[1] Martin J. Scott,[1] Richard Adair,[1] Susan Graham,[1] Ania M. Owsianka,[1] Paul Targett-Adams,[1] Kui Li,[3] Takaji Wakita,[4] John McLauchlan,[1] Stanley M. Lemon[2] and Arvind H. Patel[1]

Correspondence
Arvind H. Patel
a.patel@mrcvu.gla.ac.uk

[1]MRC Virology Unit, Institute of Virology, University of Glasgow, Church Street, Glasgow G11 5JR, UK

[2]Center for Hepatitis Research, Institute for Human Infections & Immunity, and the Department of Microbiology and Immunology, University of Texas Medical Branch, Galveston, TX 77555-0610, USA

[3]Department of Molecular Sciences, University of Tennessee Health Science Center, Memphis, TN 38163, USA

[4]Department of Virology II, National Institute of Infectious Diseases, Tokyo, Japan

The cellular DEAD-box protein DDX3 was recently shown to be essential for hepatitis C virus (HCV) replication. Prior to that, we had reported that HCV core binds to DDX3 in yeast-two hybrid and transient transfection assays. Here, we confirm by co-immunoprecipitation that this interaction occurs in cells replicating the JFH1 virus. Consistent with this result, immunofluorescence staining of infected cells revealed a dramatic redistribution of cytoplasmic DDX3 by core protein to the virus assembly sites around lipid droplets. Given this close association of DDX3 with core and lipid droplets, and its involvement in virus replication, we investigated the importance of this host factor in the virus life cycle. Mutagenesis studies located a single amino acid in the N-terminal domain of JFH1 core that when changed to alanine significantly abrogated this interaction. Surprisingly, this mutation did not alter infectious virus production and RNA replication, indicating that the core–DDX3 interaction is dispensable in the HCV life cycle. Consistent with previous studies, siRNA-led knockdown of DDX3 lowered virus production and RNA replication levels of both WT JFH1 and the mutant virus unable to bind DDX3. Thus, our study shows for the first time that the requirement of DDX3 for HCV replication is unrelated to its interaction with the viral core protein.

INTRODUCTION

Persistent hepatitis C virus (HCV) infection is a major cause of chronic hepatitis, cirrhosis and hepatocellular carcinoma (HCC). Current treatments for chronic infection are ineffective in approximately 50 % of patients (Chen & Morgan, 2006). The virus, which belongs to the family *Flaviviridae*, has a positive-sense RNA genome encoding a polyprotein that is cleaved by cellular and viral proteases to yield mature structural and non-structural proteins. The structural proteins are core and the envelope glycoproteins E1 and E2, while the non-structural proteins are p7, NS2, NS3, NS4A, NS4B, NS5A and NS5B (reviewed by Moradpour *et al.*, 2007). HCV exhibits a high degree of genetic variability with six distinct viral genotypes, each further divided into subtypes, and within a single individual the virus exists as a constantly evolving quasispecies (Bukh *et al.*, 1995; Pawlotsky, 2003; Simmonds, 1995).

HCV core is a highly conserved basic, RNA-binding protein that forms the viral nucleocapsid (McLauchlan, 2000). Mature core is a dimeric, alpha-helical protein that can be separated into two domains (D1 and D2) based on its hydropathic profile (Boulant *et al.*, 2005; McLauchlan, 2000). The N-terminal hydrophilic D1 domain consists of the first 117 aa and is mainly involved in RNA binding and oligomerization of the core protein (Boulant *et al.*, 2005).

Supplementary figures are available with the online version of this paper.

In addition, D1 also interacts with several cellular factors (McLauchlan, 2000). The hydrophobic D2 domain, which spans amino acid residues 118 to approximately 169, is required for correct folding of D1. D2 consists of two amphipathic α-helices connected by a hydrophobic loop and mediates core association with lipid droplets (LDs) and endoplasmic reticulum membranes (Barba et al., 1997; Boulant et al., 2006; Hope & McLauchlan, 2000). Recent evidence strongly suggests that the HCV core–LD association is important for the production of infectious virus particles (Boulant et al., 2007; Miyanari et al., 2007; Shavinskaya et al., 2007).

We and others previously showed that the core domain D1 interacts with the cellular DEAD-box RNA helicase DDX3 (Mamiya & Worman, 1999; Owsianka & Patel, 1999; You et al., 1999). In mammalian cells, DDX3 is present throughout the cytoplasm and can also be found in the nucleus. Ectopic expression of HCV core in these cells results in the redistribution of a proportion of DDX3 to distinct cytoplasmic sites, where it co-localizes with core. Indeed, DDX3 was recently shown to be present on LDs in core-expressing Hep39 cells (Sato et al., 2006).

Cellular RNA helicases of the DEAD-box family participate in all biological processes involving RNA. They possess nine conserved motifs (see Fig. 1), including motif II (Asp–Glu–Ala–Asp or DEAD) after which the protein family is named (reviewed by Cordin et al., 2006; Rocak & Linder, 2004). DDX3 is a ubiquitous cellular protein, possessing ATPase and helicase activities (Franca et al., 2007; Yedavalli et al., 2004). Known homologues include murine PL10 (Leroy et al., 1989), Xenopus laevis An3 (Gururajan et al., 1991) and yeast Ded1 (Jamieson & Beggs, 1991). The exact cellular function of DDX3 has yet to be defined, but there is evidence for its involvement in splicing (Deckert et al.,

2006; Zhou et al., 2002), translation initiation and repression (Beckham et al., 2008; Shih et al., 2008), cell cycle regulation (Chang et al., 2006; Chao et al., 2006; Huang et al., 2004; Sekiguchi et al., 2007), nucleo-cytoplasmic RNA shuttling (Yedavalli et al., 2004), RNA transport (Kanai et al., 2004), interferon induction (Schroder et al., 2008; Soulat et al., 2008) and apoptosis (Sun et al., 2008). Both upregulation and downregulation of DDX3 have been reported in various tumour tissues, suggesting divergent roles of DDX3 in cancer-related pathogenesis (Botlagunta et al., 2008; Chang et al., 2006; Chao et al., 2006; Huang et al., 2004).

Previously, we proposed that the HCV core–DDX3 interaction might function in virus replication and/or pathogenesis (Owsianka & Patel, 1999). Two separate studies recently provided evidence for the involvement of DDX3 in HCV replication (Ariumi et al., 2007; Randall et al., 2007). The importance of DDX3 in the life cycle of other viruses has also become apparent, including its requirement for human immunodeficiency virus-1 (HIV-1) replication (Yedavalli et al., 2004). Furthermore, the DDX3 homologue Ded1 is required for brome mosaic virus replication (Noueiry et al., 2000). In contrast, DDX3 inhibits hepatitis B virus transcription by its incorporation into nucleocapsids (Wang et al., 2009). Thus, there is increasing evidence that DDX3 is important in the life cycle of several diverse viruses.

The direct relevance of the core–DDX3 interaction for the HCV life cycle has not yet been elucidated. In this study, we show that this interaction does occur in cultured cells infected with HCV strain JFH1 (Wakita et al., 2005), and that DDX3 co-localizes directly with core on LDs. Using alanine substitution mutagenesis, we identified a key amino acid residue within the D1 domain of core that is
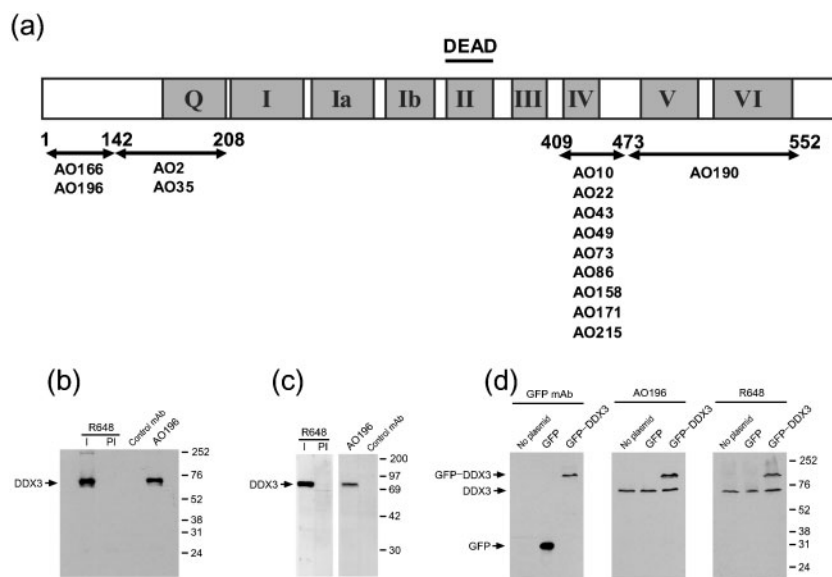
Fig. 1. Generation of anti-DDX3 antibodies. (a) Schematic representation of DDX3 protein structure showing the nine conserved motifs, including motif II (or the DEAD motif). The arrows mark the epitopes recognized by the mouse mAbs. (b) Characterization of anti-DDX3 antibodies. HuH-7 cell lysates were immunoprecipitated with the immune (I) and pre-immune (PI) antiserum R648, or mAb AO196 or an isotype control mAb. The immune complexes were analysed by Western blotting using biotinylated R648. Positions of molecular mass markers are shown (in kDa). (c) Western blotting of HuH-7 cell lysates with R648-I, -PI, mAb AO196 and isotype control mAb. (d) Western blotting of lysates of HEK cells transfected with a plasmid expressing EGFP alone or an EGFP–DDX3 fusion protein using anti-GFP mAb, AO196 and R648.

critical for this interaction. Furthermore, we examine the impact of abrogation of the core–DDX3 interaction on virus RNA replication and infectious progeny yields in cultured cells.

RESULTS

Generation of DDX3 antibodies

We previously showed that DDX3 co-localizes with HCV genotype 1a core in cytoplasmic punctate spots (Owsianka & Patel, 1999). To better understand the nature of this interaction, we generated several mouse mAbs (prefixed with 'AO', see Fig. 1a) and two rabbit polyclonal antisera (R647 and R648) to human DDX3. Both rabbit antisera and the majority of mAbs were found to interact with DDX3 by ELISA, Western blotting and immunoprecipitation assays (data not shown). The epitopes of mAbs reactive to DDX3 in Western blots were broadly mapped using truncated forms of DDX3 expressed in bacteria as GST-fusion proteins. Most of the mAbs recognized aa 409–473, a region located between motifs III and V of DDX3,

whereas mAb AO190 recognized motifs V and VI. mAbs AO166 and AO196 bound to the N-terminal region, whereas mAbs AO2 and AO35 recognized the region downstream preceding the ATPase domain of DDX3 (Fig. 1a).

The specificities of antibodies AO196 and R648 for DDX3 in immunoprecipitation and Western blot assays are shown in Fig. 1(b, c, d). The polyclonal serum R648 (but not the pre-immune control serum) specifically immunoprecipitated DDX3 from a cytoplasmic extract of HuH-7 cells, as did mAb AO196 (Fig. 1b). R648 and AO196 also recognized DDX3 in cytoplasmic extracts of HuH-7 cells by Western blotting (Fig. 1c). The specificity of these antibodies was further demonstrated by their recognition of both endogenous DDX3 and an enhanced green fluorescent protein (EGFP)–DDX3 fusion protein expressed in HEK cells (Fig. 1d). mAb AO196 and R648 recognized only the cytoplasmic form of DDX3 by immunofluorescence (Fig. 2a and data not shown), even though they were able to detect DDX3 in the nuclear extracts of cells in both immunoprecipitation and Western blotting assays (data not shown). In contrast, another mAb
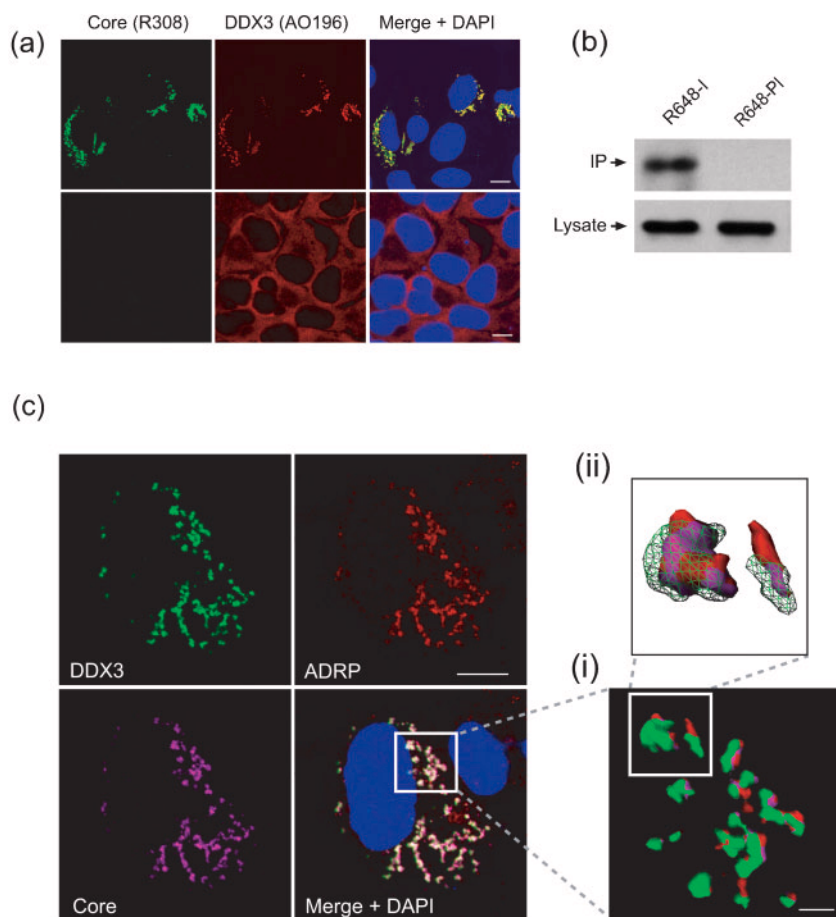
Fig. 2. Sequestration of DDX3 by HCV core. (a) DDX3 co-localizes with core in JFH1-infected cells. HuH-7 cells were either mock-infected (lower panel) or infected with JFH1 (top panel). At 3 days post-infection, cells were fixed and probed with HCV core and DDX3 using antibodies R308 and A0196, respectively. Cell nuclei were detected by counter-staining with DAPI. (b) Co-immunoprecipitation of core by anti-DDX3 antiserum. HuH-7 cells electroporated with viral RNA were lysed at 72 h post-incubation, and the lysate immuno-precipitated with anti-DDX3 R648 immune (I) or pre-immune (PI) serum. The resulting pre-cipitates were examined by immunoblotting using anti-core mAb c7-50 (top panel). One twentieth of the cell lysate used in the co-immunoprecipitation assay was immunoblotted for core with mAb c7-50 as the input control (bottom panel). (c) Localization of DDX3 and core on LDs. HuH-7 cells electroporated with the JFH1$_{WT}$ RNA were fixed at 72 h post-transfection and probed using antibodies to core (R308), DDX3 (AO196) and ADRP. Z-stack analysis of all three proteins was per-formed by recording a series of approximately 20 images. 3D reconstructions of the boxed areas are shown (i) and a selected area is shown in greater detail (ii) where DDX3 is depicted as a wire frame to reveal the core–ADRP association. Bars, 10 μm for confocal images and 2 μm for 3D image.

designated AO322 recognized both the cytoplasmic and the nuclear form of DDX3 by immunofluoresence (Supplementary Fig. S1a).

HCV core interacts with cellular DDX3 in cells replicating WT JFH1

The core–DDX3 interaction was previously demonstrated in cells ectopically expressing HCV genotype 1a core, and in the absence of virus RNA replication and productive infection (Owsianka & Patel, 1999). To test whether DDX3 interacts with JFH1 core, HuH-7 cells transfected with virus RNA were first analysed by indirect immunofluorescence. DDX3 was found to be sequestered by core in JFH1-replicating cells as detected using mAbs AO196 and AO322 [Fig. 2a and Supplementary Fig. S1a (available in JGV Online), respectively]. It should be noted that the core-bound DDX3 emitted a stronger fluorescent signal compared with free DDX3 occupying the cell cytoplasm. Thus, adjustment of the core-bound DDX3 signal to prevent overexposure resulted in the apparent loss of free DDX3 from the image. A representative image of core and DDX3 in virus-infected and surrounding non-infected cells taken at two different intensities is shown in Supplementary Fig. S1(b) (available in JGV Online). The anti-DDX3 antiserum R648 specifically co-immunoprecipitated core from JFH1-replicating cells, further confirming a direct interaction between these two proteins (Fig. 2b).

We also found that DDX3 co-localized with core protein in the NNeo/C-5B(+) cell line harbouring an autonomously replicating genome-length genotype 1b RNA (Ikeda et al., 2002), and HuH-7 cells infected with the intergenotypic 1a/2a chimeric virus [H-NS2/NS3 J(YH/QL)] (Yi et al., 2007) (Supplementary Fig. S1c, d, available in JGV Online). Thus, the recruitment of DDX3 by core is in good agreement with our previous results (Owsianka & Patel, 1999), and is not limited to one virus genotype.

DDX3 interacts with HCV core on LDs

The association of HCV core with LDs is essential for infectious virus production (Boulant et al., 2007; Miyanari et al., 2007; Shavinskaya et al., 2007). We sought to gain further insight into the core–DDX3 complex in the context of the JFH1 system by analysing the intracellular distribution of core and DDX3. HuH-7 cells electroporated with JFH1 RNA were analysed by indirect immunofluorescence for HCV core, DDX3 and adipocyte differentiation-related protein (ADRP), a protein abundant on the surface of LDs (Fujimoto et al., 2004). As shown in Fig. 2(c) left, core associated with ADRP and the localization of DDX3 was precisely coincident with both proteins, indicating its redistribution to LDs. To examine the subcellular position of DDX3 and core in relation to ADRP in greater detail, a series of Z-stacks was obtained and used after blind deconvolution to create a three-dimensional model of LDs

coated by core, ADRP and DDX3. As reported before (Boulant et al., 2007), core fully coated LDs. We found that DDX3 by virtue of its interaction with core was also fully associated with LDs [Fig. 2c (i) and (ii)].

Identification of core residues required for DDX3 interaction

We previously reported that aa 1–59 of core protein are involved in its interaction with DDX3 (Owsianka & Patel, 1999). To identify critical residues within this region, a library of core 1–59 mutants containing single or multiple amino acid substitutions was generated by error-prone PCR (EP-PCR). The mutated sequences were fused in-frame with GFP and expressed in bacteria. The mutant fusion proteins were screened by incubation with GST–DDX3 fusion protein immobilized in ELISA wells, and the bound mutants detected using a rabbit polyclonal anti-GFP antiserum. Of 130 clones screened, only nine were found to be defective in binding to GST–DDX3 (data not shown). In order to confirm these results, all nine mutants were individually subcloned into a sequence encoding the HCV genotype 1a strain H77c core, E1 and E2 (pCE1E2) in a mammalian expression vector pcDNA3.1/Zeo+ (Invitrogen), and their expression was analysed by indirect immunofluorescence. The results were in accordance with the data from the initial ELISA screen in that all nine mutated core proteins failed to redistribute DDX3 (data not shown). Nucleotide sequence analysis showed that each of the mutants carried between one and four amino acid substitutions (Fig. 3). Of interest, mutant 90 had only one substitution (I30N), indicating that this residue must be required for the interaction of core with DDX3. All nine mutant proteins had at least one amino acid substitution in the region spanning residues 24–36, indicating that this region may harbour residues that are critical for the core–DDX3 interaction. To test this hypothesis, site-directed mutagenesis was carried out to revert any mutations outside of this 13 aa region back to the WT residue. These new mutant core 1–59 fragments were then subcloned into pCE1E2, and their expression analysed following transient transfection into HuH-7 cells as above. Again, none of these new core mutants redistributed DDX3 (data not shown), indicating that the 13 aa region between residues 24 and 36 of core is indeed involved in the interaction between core and DDX3. To determine which residues in this 13 aa region were essential, we carried out alanine-scanning mutagenesis across aa 24–36, individually substituting each residue in this region with alanine. As before, these alanine mutant sequences were subcloned into pCE1E2 and transiently transfected into HuH-7 cells. Immunofluorescence analysis revealed seven mutants (P25A, G26A, G28A, Q29A, V31A, G32A and L36A) that showed distinct co-localization between core and DDX3 (similar to that seen with WT HCV core), whilst the other mutants (F24A, G27A, I30A, G33A, V34A and Y35A) displayed no interaction with DDX3 at all (Supplementary Fig. S2, available in JGV Online). Thus, these results

```
                 1        10        20        30        40        50      59
Core      MSTNPKPQPK TKRNTNRRPE DVKFPGGGQI VGGVYLLPRR GPRLGVRTTR KTSERSQPR
Mutant 25 --------K- ---------- ---------- ---G------ ---------- ------R--
Mutant 36 ---------- ---------- ---------- ---D----W- ---------- -S-------
Mutant 90 ---------- ---------- --------N- ---D------ ---------- ---------
Mutant 99 ---------- ---------- -D-------- ---D------ ---------- ---------
Mutant 110 ---------- ---------- --------N- ---------- --S------- ---------
Mutant 111 -----E---- ---------- ---------- ----N----- ---------- ---------
Mutant 115 --------D -E-------- ---S------ ---------- ---------- ---------
Mutant 125 ---------- -----I---- --------R- ----N----- ---------- ------R--
Mutant 126 -------H-- ---------- -----D---N -----W---- ---------- ---------
```

Fig. 3. Identification of core residues critical for its interaction with DDX3. Amino acid substitutions in residues 1–59 of core in nine mutants unable to interact with DDX3. Residues in the region 24–36 (shaded box) were targeted for alanine-scanning mutagenesis, which identified residues at positions 24, 27, 30, 33, 34 and 35 (underlined in the sequence at the top) that were critical for DDX3 interaction.

indicate that core residues F24, G27, I30, G33, V34 and Y35 are critical for its interaction with DDX3.

Disrupting the core–DDX3 interaction

Sequence comparison of core protein from strains H77c (genotype 1a) and JFH1 (genotype 2a) revealed 96.6 % identity within the first 59 residues of core, with the key residues (F24, G27, I30, G33, V34 and Y35) for interaction with DDX3 being fully conserved (data not shown). Thus, recombinant JFH1 genomes each containing one of the six mutations were constructed. All mutants were replication competent as seen by the expression of NS5A protein at 3 days post-transfection (Fig. 4). The viral core protein in these cells was detected using two different anti-core antibodies, which bound to the mutant proteins with

Fig. 4. Analysis of JFH1 core mutant viruses. HuH-7 cells electroporated with viral RNAs as shown were subjected to Western immunoblotting at 72 h post-incubation using anti-NS5a mAb 9E10, anti-core antibodies mAb c7-50 or R308, anti-DDX3 mAb AO196 and an anti-tubulin antibody.

varying affinity. mAb c7-50 bound minimally or not at all to I30A and G33A mutants, but had increased affinity for the V34A protein. The anti-core rabbit serum R308 on the other hand recognized all core forms equally except for G33A (Fig. 4). Notably, all six core mutations are located within the epitope (aa 21–40) recognized by c7-50 (Moradpour et al., 1996), which may account for the altered affinity of this mAb to some mutants. The antiserum R308 was raised against a peptide corresponding to core aa 5–25 (Hope & McLauchlan, 2000). Therefore, the smaller quantities of G33A core detected using R308 suggest either this mutation lowers the stability of the protein or simply reduces the binding efficiency of the antibody. Importantly, there was no detectable change in DDX3 protein levels in any of the transfected cell cultures tested (Fig. 4).
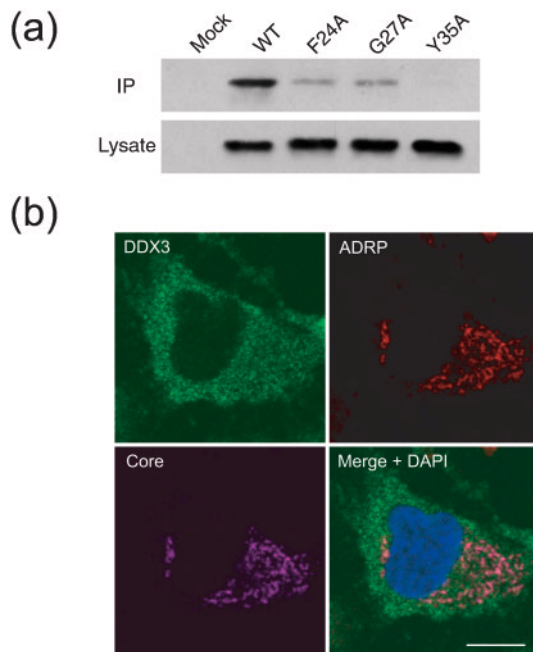
We next tested by co-immunoprecipitation if these mutations had effectively disrupted the core–DDX3 interaction in virus-replicating cells. We excluded mutants I30A, G33A and V34A from this assay due to their altered affinity to mAb c7-50 (Fig. 4), which is the antibody we found to be most compatible in our co-immunoprecipitation assay. As shown in Fig. 5, the F24A and G27A core mutants were co-immunoprecipitated by the anti-DDX3 antiserum R648 in much lower amounts than the WT protein. However, the Y35A core was not co-immunoprecipitated at all, indicating that its interaction with DDX3 was abrogated. Consistent with these findings, no co-localization of core and DDX3 was seen in cells replicating JFH1$_{Y35A}$ by immunofluoresence analysis (Fig. 5b). Importantly, this mutant core remained associated with LDs, which is not surprising since motifs responsible for targeting core to LDs are located in the D2 domain (Hope & McLauchlan, 2000).
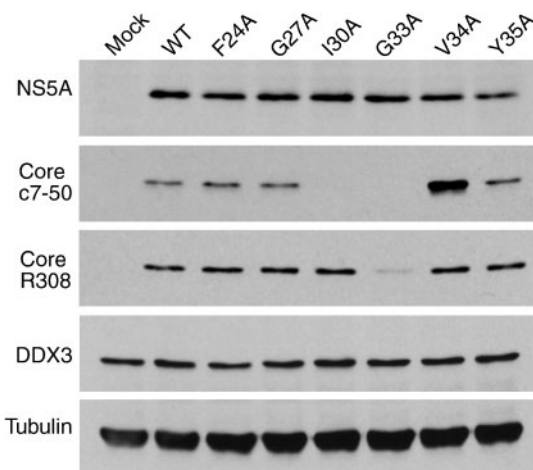
HCV replication in the absence of the core–DDX3 interaction

To determine the importance of this interaction in the virus life cycle, we examined the phenotype of JFH1$_{Y35A}$.

Fig. 5. Analysis of the interaction of DDX3 with core mutants. (a) HuH-7 cells were electroporated with different viral RNAs and HCV core co-immunoprecipitated at 72 h post-incubation using the anti-DDX3 serum R648 as described in the legend to Fig. 2b. (b) HuH-7 cells electroporated with JFH1$_{Y35A}$ were fixed at 72 h post-incubation and analysed by confocal microscopy for the intracellular distribution of core, DDX3 and ADRP using appropriate antibodies. Bar, 10 μm.

HuH-7 cells were electroporated with JFH1$_{WT}$, JFH1$_{Y35A}$ or the replication-deficient JFH1$_{GND}$ RNAs and incubated for various time points before determining the progeny virus yields released into the medium and intracellular viral RNA levels. As shown in Fig. 6(a), the number of infectious particles released by JFH1$_{Y35A}$-replicating cells was lower in comparison with JFH1$_{WT}$-transfected cells at 24 and 48 h post-transfection, although parity was achieved at 72 h. The intracellular RNA replication levels of JFH1$_{Y35A}$ were similar to JFH1$_{WT}$ throughout the time-course (Fig. 6b). As expected, no virus release or intracellular viral RNA replication was detected in cells harbouring JFH1$_{GND}$ RNA (Fig. 6a, b). We next examined the infectivity and replication of the core mutant virus released from electroporated cells. To do this, we infected naïve cells at an equal m.o.i. and quantified the released infectious virus progeny and the intracellular viral RNA at various times post-infection. As shown in Fig. 6(c, d), respectively, both the virus yields and RNA replication levels of JFH1$_{Y35A}$ were very similar to JFH1$_{WT}$. We found no direct reversion or second-site mutation in JFH1$_{Y35A}$ core sequence. Thus, our data indicate that the core–DDX3 interaction does not play a role in HCV morphogenesis.

Replication of HCV following siRNA-mediated knockdown of DDX3

Recent reports have shown that siRNA-mediated knockdown of DDX3 reduces JFH1$_{WT}$ replication in infected cells (Ariumi et al., 2007; Randall et al., 2007). To assess the influence of DDX3 abundance on virus infection in the absence of the core–DDX3 interaction, we measured the replication of JFH1$_{WT}$ and JFH1$_{Y35A}$ following infection of
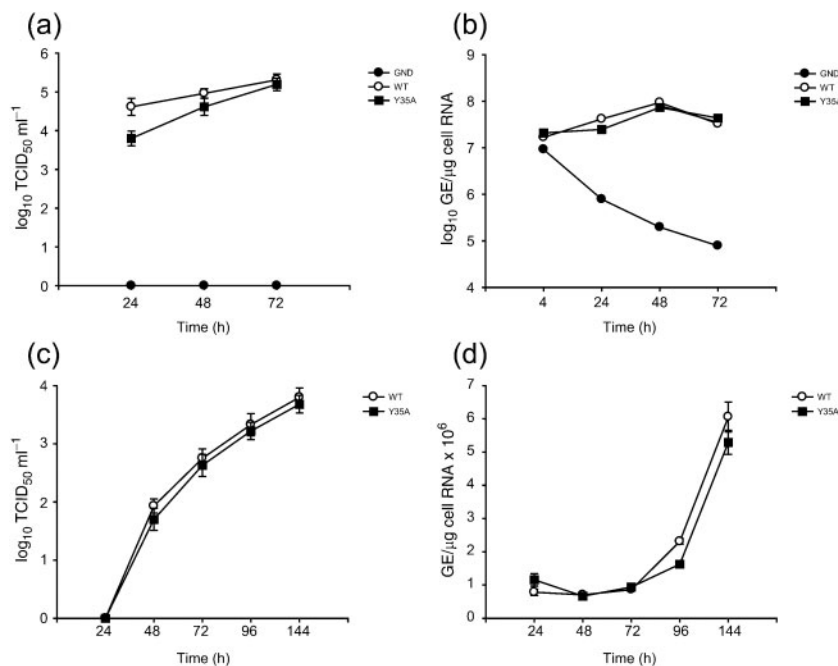
Fig. 6. Analysis of the core mutant viruses. (a, b) Determination of virus yield and intracellular RNA levels following transfection. HuH-7 cells were electroporated with RNA derived from JFH1$_{WT}$, JFH1$_{Y35A}$ or JFH1$_{GND}$ cDNA. At the indicated time points (a) the released virus titres and (b) the intracellular HCV RNA levels were quantified by TCID$_{50}$ and RT-qPCR, respectively. (c and d) Determination of virus yield and intracellular RNA levels following infection. Naïve HuH-7 cells were infected with JFH1$_{WT}$ or JFH1$_{Y35A}$ (obtained from the electroporated cells above) at an m.o.i. of 0.02. The (c) titres of infectious virus released into the medium and (d) intracellular viral RNA levels were measured over 6 days as described above. Means and error ranges from duplicate electroporations and infections are shown.

cells that had undergone efficient siRNA knockdown of DDX3 (Fig. 7a). As previously described, DDX3 knockdown cells were substantially less permissive for virus replication than normal cells following infection with JFH1$_{WT}$. Similar reductions in JFH1$_{Y35A}$ replication levels were also observed (Fig. 7b). Collectively, the data presented in Figs 6 and 7 indicate that DDX3 promotes efficient HCV infection by processes that are independent of its interaction with the viral core protein.

DISCUSSION

The recent advent of the HCV cell culture system has enabled us to further characterize the core–DDX3 interaction in the context of the complete HCV life cycle. Our overall goal is to deduce the role of DDX3 in normal cells with a view to understanding the significance of its interaction with HCV core in the virus life cycle and pathogenesis. Towards this end, we generated a large panel of mAbs recognizing different regions of DDX3. Using a subset of these, we confirmed that this interaction is genuine in JFH1-infected cells.

Given the putative function of DDX3 in RNA metabolism, initial identification of the core–DDX3 interaction led us and others to postulate its possible role in virus replication and assembly (Mamiya & Worman, 1999; Owsianka & Patel, 1999; You et al., 1999). Recent data using the JFH1 system suggest that HCV RNA replication and virus assembly occur in LD-associated membranes (Boulant et al., 2007; Miyanari et al., 2007). Core protein, which associates with LDs (McLauchlan, 2000; Roingeard & Hourioux, 2008), recruits the viral non-structural proteins, replication complexes and envelope glycoproteins to these sites, allowing virus assembly to proceed in this local environment (Miyanari et al., 2007). We show here that core also recruits the cellular DDX3 to LDs, suggesting that it may have a function in HCV replication. In keeping with this, two recent studies have shown reductions in JFH1 replication when DDX3 is removed from the cell by siRNA (Ariumi et al., 2007; Randall et al., 2007). We hypothesized that disrupting the association between HCV core and DDX3 might be detrimental to HCV replication, and provide insights into the purpose of this interaction. Our mutagenesis analysis revealed that the Y35A substitution in the JFH1 core molecule abrogated this interaction without affecting core–LD association. No alteration to virus RNA replication, translation or infectious particle production was observed following transfection of this mutant viral RNA into the cells. Similarly, JFH1$_{Y35A}$ virus yields from cells infected with the mutant progeny were equivalent to those of the WT virus. Interestingly, the two other mutants identified in this study (JFH1$_{F24A}$ and JFH1$_{G27A}$) showed greater reductions in virus replication, particularly post-infection (Supplementary Fig. S3, available in JGV Online). However, given their interaction with DDX3 is only slightly reduced (Fig. 5), this impairment is unlikely to be related to the disruption of the core–DDX3 interaction. A more plausible explanation for their unusual phenotypes could be an alteration in core function and/or RNA structure resulting from an alanine substitution at these positions, and as such these mutants require further investigations. Nevertheless, our results collectively suggest that the core–DDX3 interaction plays no role in virus morphogenesis.

Subgenomic replicons that do not possess core replicate as well as, if not better than, replicons encoding the entire polyprotein (Blight et al., 2000; Ikeda et al., 2002; Lohmann et al., 1999), which indicates that the core–DDX3 interaction per se is not essential for HCV RNA replication. Nevertheless, Ariumi et al. (2007) reported that subgenomic replicons showed a twofold decrease in RNA replication in DDX3 knockdown cells. This finding raises an intriguing prospect that DDX3 may play a direct role in HCV RNA replication independent of and in addition to its interaction with core. Nonetheless, these workers observed a much greater reduction in JFH1 RNA replication in cells supporting replication of full genome-length RNAs, indicating greater importance of DDX3 in this setting and supporting the functional relevance of the interaction of DDX3 with core. We reproduced the deleterious effects of DDX3 knockdown on the JFH1$_{WT}$ replication but also found a similar phenotype for JFH1$_{Y35A}$ (Fig. 7). This finding further supports the notion of the core–DDX3 interaction having no function in HCV replication. Therefore, our data make a clear distinction between the effects of siRNA knockdown of DDX3 from the cells and disruption of the core–DDX3 interaction on HCV replication.

The possible involvement of the core–DDX3 interaction in pathogenesis cannot be discounted. Indeed, core protein has been widely implicated in modulating cellular functions, mainly due to its interaction with numerous host
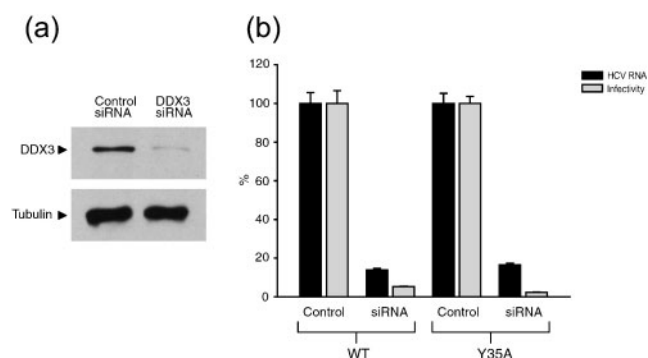
Fig. 7. Infection of DDX3 knockdown cells. (a) HuH-7 cells were transfected with siRNA duplexes as indicated. Cells were harvested after 2 days and examined by Western blotting using the anti-DDX3 mAb AO196. (b) Naïve and DDX3-deficient HuH-7 cells were infected with WT JFH1$_{WT}$ or JFH1$_{Y35A}$ virus. At 2 days post-infection the levels of released virus and intracellular HCV RNA were measured by TCID$_{50}$ assay and RT-qPCR, respectively. Means and error ranges from duplicate infections are shown.

factors (McLauchlan, 2000; Ray & Ray, 2001; Watashi & Shimotohno, 2003). Differential regulation of DDX3 has been reported in a number of tumours, including HCC, suggesting that it may be involved in HCV-associated pathogenesis (Botlagunta *et al.*, 2008; Chang *et al.*, 2006; Chao *et al.*, 2006; Huang *et al.*, 2004). DDX3 is also one of several DEAD-box proteins that are upregulated during HIV-1 replication (Krishnan & Zeichner, 2004). Interestingly, it is also upregulated during immune response to lipopolysaccharide-induced inflammation and during interferon treatment (de Veer *et al.*, 2001; Saban *et al.*, 2006). Thus, it is possible that during active viral replication HCV recruits DDX3 protein to evade host immune recognition, thereby adversely affecting one or more of its roles in normal cells (Rosner & Rinkevich, 2007) and in turn contributing to viral pathogenesis. Although we observed no differences in DDX3 expression levels between JFH1-infected cultured cells and uninfected cells, its relevance *in vivo* from a long-term disease perspective warrants further investigation.

METHODS

Cell culture and antibodies. Human hepatoma HuH-7 (Nakabayashi *et al.*, 1982) cells were propagated as described previously (Witteveldt *et al.*, 2009). The anti-NS5A mouse monoclonal antibody (mAb) 9E10 was a kind gift from Charles M. Rice (Center for the Study of Hepatitis C, The Rockefeller University, New York, USA) (Lindenbach *et al.*, 2005). The anti-HCV core rabbit serum R308, and the anti-ADRP sheep serum have been described previously (Hope & McLauchlan, 2000; Targett-Adams *et al.*, 2003). The anti-HCV core mAb c7-50 and the anti-α-tubulin and anti-GFP mAbs were purchased from Bioreagents and Sigma, respectively.

Generation and characterization of anti-DDX3 antibodies. BALB/c mice and rabbits were immunized with a bacterially expressed glutathione *S*-transferase-full-length DDX3 (GST–DDX3) fusion protein and antibodies generated essentially as previously described (Clayton *et al.*, 2002). A total of two rabbit polyclonal antisera (R647 and R648) and 16 mouse hybridomas secreting mAbs (see Fig. 1) to DDX3 was generated. The mAbs were initially identified and selected on the basis of their ability to interact with GST–DDX3, but not an irrelevant GST fusion protein, in an ELISA assay (data not shown).

Plasmid constructs and mutagenesis. The full-length DDX3 gene was cloned into the *Bam*HI site, in-frame to sequences encoding the EGFP, in the vector pEGFP-C1 (Clontech) to generate EGFP–DDX3 fusion protein.

To identify residues within the N-terminal 59 aa of HCV core that are critical for interaction with DDX3, EP-PCR was performed to introduce random mutations into the HCV genotype 1a strain H77c (Yanagi *et al.*, 1997) sequence encoding this region. The fidelity of *Taq* polymerase was decreased by altering the relative dNTP concentrations, using a high Mg^{2+} concentration and including Mn^{2+} in the reaction as described previously (Pritchard *et al.*, 2005). The mutated sequences were cloned in-frame with (and downstream of) green fluorescence protein (GFP) in the bacterial expression vector pKK223-3 (Pharmacia) and the library of core 1–59 mutant–GFP fusion proteins generated was screened in an *in vitro* DDX3-binding assay as described in Results. Nucleotide sequencing subsequently identified the mutations introduced by EP-PCR in the clones of interest.

The plasmid pUC-JFH1 carries the full-length cDNA of the genotype 2a HCV strain JFH1 (Wakita *et al.*, 2005). The plasmids pUC-GND JFH1 and pUC-JFH1 ΔE1E2 are identical except that they carry the GND mutation in the NS5B-encoding sequence, or an in-frame deletion in the E1 and E2 sequences (Wakita *et al.*, 2005). Site-directed mutagenesis was carried out using the QuikChange-II kit (Stratagene) to introduce alanine substitutions at the target sites in core. Briefly, various alanine substitutions in the core-coding region were individually introduced into the plasmid pGEM-T (Promega) carrying nt 1–2614 (corresponding to the 5′ UTR and core to E2 coding sequence) of HCV strain JFH1 using appropriate primers (the sequences of which are available upon request). The presence of the desired mutation in the resulting clones was confirmed by nucleotide sequencing. Sequences carrying the appropriate mutation were subcloned back into pJFH1-pUC to generate mutant viruses (see below).

Generation of JFH1 virus and its mutated derivatives. Ten micrograms of RNA synthesized *in vitro* using linearized plasmid templates carrying the wild-type (WT) or mutated JFH1 genomic cDNA was electroporated into HuH-7 cells as described previously (Wakita *et al.*, 2005). The electroporated cells were seeded into appropriate tissue culture dishes and incubated at 37 °C. At the indicated time period, the medium containing the infectious virus progeny was filtered through a 0.45 μm pore-sized membrane and infectivity determined as described below.

Determination of virus infectivity and RNA replication. Virus titres in the culture supernatants were determined as $TCID_{50}$ (Lindenbach *et al.*, 2005) following immunostaining for NS5A. The intracellular and extracellular HCV RNA content was measured by reverse transcription-quantitative real-time-polymerase chain reaction (RT-qPCR) as described previously (Witteveldt *et al.*, 2009). To determine virus replication after electroporation, cells transfected with the respective transcript were seeded into 10 cm culture dishes, incubated at 37 °C for 4 h and then trypsinized. Total RNA was prepared from 1/15 of the trypsinized cells using the RNeasy kit (Qiagen) to quantify viral RNA by qRT-PCR assay. The remaining cell suspension was split 1:3 into three T25 flasks. Following incubation at 37 °C for 24, 48 and 72 h, the infectious virus yields in cell culture supernatants were determined by $TCID_{50}$ assay and the intracellular viral RNA levels quantified by RT-qPCR. To measure virus replication after infection, 5.3×10^3 naïve HuH-7 cells seeded into six-well culture dishes were infected with virus at the indicated m.o.i. Following incubation at 37 °C for 24, 48, 72, 96 and 144 h, infectious virus yields and intracellular viral RNA levels were determined as described above.

SDS-PAGE and Western blotting. Cell lysates were subjected to SDS-PAGE followed by Western blotting using appropriate antibodies as described previously (Clayton *et al.*, 2002). The bound antibodies were detected using enhanced chemiluminescence reagents (Amersham).

Immunoprecipitation of DDX3. HuH-7 cells were washed with PBS, lysed in lysis buffer (20 mM Tris/HCl pH 7.4, 20 mM iodoacetamide, 150 mM NaCl, 1 mM EDTA and 0.5 % Triton X-100) and the lysate was spun briefly to remove nuclei. The clarified cell lysates were incubated with the anti-DDX3 antibodies as described in the text and the immune complexes precipitated using protein G agarose beads (Sigma). Following washes of the Sepharose beads, the immune complexes were analysed by SDS-PAGE followed by Western blotting using biotinylated R648 and anti-streptavidin-horseradish peroxidase (HRP) conjugate.

Co-immunoprecipitation of HCV core protein. Approximately, 5×10^6 HuH-7 cells electroporated with viral RNA were seeded into

100 mm tissue culture dishes. At 72 h post-transfection, the cells were washed and lysed in 0.5 ml lysis buffer (20 mM Tris/HCl, pH 7.4, 135 mM NaCl and 0.1 % Triton X-100) supplemented with 50 mM NAF, 5 mM Na$_3$VO$_4$ and 1 mM PMSF. The lysate was spun briefly to remove nuclei. After pre-clearing, the clarified lysate was immuno-precipitated overnight with protein G agarose beads that had been pre-incubated with the anti-DDX3 antiserum R648. The beads carrying the immune complex were spun at 2000 r.p.m. (microcen-trifuge) for 2 min, washed three times with the lysis buffer and subjected to non-reducing SDS-PAGE followed by Western blotting using the anti-core mAb c7-50 and anti-mouse IgG-HRP conjugate.

Indirect immunofluorescence. Cells on coverslips were fixed in methanol and probed with the indicated primary antibody for 1 h at room temperature. After washing with PBS, cells were incubated with anti-species antibodies conjugated with fluorescein isothiocyanate, tetramethyl rhodamine isothiocyanate or Cy5 (Invitrogen) for 1 h and then washed with PBS. The coverslips were examined with a Zeiss Laser Scanning LSM510 META inverted confocal microscope (Carl Zeiss) and the images analysed using LSM510 software. Three-dimensional (3D) reconstructions were performed from Z-stack images collected using optimum intervals. Image stacks were deconvolved by 3D-blind deconvolution using Autodeblur software (MediaCybernetics), and 3D reconstructions were generated as described previously (Boulant *et al.*, 2007; Targett-Adams *et al.*, 2008).

RNA interference. Two pre-validated siRNA duplexes (s4004 and s4005, synthesized by Applied Biosystems) targeting different regions of the human DDX3 and a negative control siRNA composed of a scrambled sequence were used. Naïve HuH-7 cells plated overnight were transfected with lipofectamine RNAiMax (Invitrogen) and 50 nM siRNAs according to the manufacturer's protocol. The cells were then incubated for a further 2 days prior to virus infection. The efficiency of DDX3 knockdown was determined by immunoblotting using mAb AO196.

ACKNOWLEDGEMENTS

REFERENCES

Ariumi, Y., Kuroki, M., Abe, K., Dansako, H., Ikeda, M., Wakita, T. & Kato, N. (2007). DDX3 DEAD-box RNA helicase is required for hepatitis C virus RNA replication. *J Virol* **81**, 13922–13926.

Barba, G., Harper, F., Harada, T., Kohara, M., Goulinet, S., Matsuura, Y., Eder, G., Schaff, Z., Chapman, M. J. & other authors (1997). Hepatitis C virus core protein shows a cytoplasmic localization and associates to cellular lipid storage droplets. *Proc Natl Acad Sci U S A* **94**, 1200–1205.

Beckham, C., Hilliker, A., Cziko, A. M., Noueiry, A., Ramaswami, M. & Parker, R. (2008). The DEAD-Box RNA helicase Ded1p affects and accumulates in *Saccharomyces cerevisiae* P-bodies. *Mol Biol Cell* **19**, 984–993.

Blight, K. J., Kolykhalov, A. A. & Rice, C. M. (2000). Efficient initiation of HCV RNA replication in cell culture. *Science* **290**, 1972–1974.

Botlagunta, M., Vesuna, F., Mironchik, Y., Raman, A., Lisok, A., Winnard, P., Jr, Mukadam, S., Van Diest, P., Chen, J. H. & other authors (2008). Oncogenic role of DDX3 in breast cancer biogenesis. *Oncogene* **27**, 3912–3922.

Boulant, S., Vanbelle, C., Ebel, C., Penin, F. & Lavergne, J. P. (2005). Hepatitis C virus core protein is a dimeric alpha-helical protein exhibiting membrane protein features. *J Virol* **79**, 11353–11365.

Boulant, S., Montserret, R., Hope, R. G., Ratinier, M., Targett-Adams, P., Lavergne, J. P., Penin, F. & McLauchlan, J. (2006). Structural determinants that target the hepatitis C virus core protein to lipid droplets. *J Biol Chem* **281**, 22236–22247.

Boulant, S., Targett-Adams, P. & McLauchlan, J. (2007). Disrupting the association of hepatitis C virus core protein with lipid droplets correlates with a loss in production of infectious virus. *J Gen Virol* **88**, 2204–2213.

Bukh, J., Miller, R. H. & Purcell, R. H. (1995). Genetic heterogeneity of hepatitis C virus: quasispecies and genotypes. *Semin Liver Dis* **15**, 41–63.

Chang, P. C., Chi, C. W., Chau, G. Y., Li, F. Y., Tsai, Y. H., Wu, J. C. & Wu Lee, Y. H. (2006). DDX3, a DEAD box RNA helicase, is deregulated in hepatitis virus-associated hepatocellular carcinoma and is involved in cell growth control. *Oncogene* **25**, 1991–2003.

Chao, C. H., Chen, C. M., Cheng, P. L., Shih, J. W., Tsou, A. P. & Lee, Y. H. (2006). DDX3, a DEAD box RNA helicase with tumor growth-suppressive property and transcriptional regulation activity of the p21waf1/cip1 promoter, is a candidate tumor suppressor. *Cancer Res* **66**, 6579–6588.

Chen, S. L. & Morgan, T. R. (2006). The natural history of hepatitis C virus (HCV) infection. *Int J Med Sci* **3**, 47–52.

Clayton, R. F., Owsianka, A., Aitken, J., Graham, S., Bhella, D. & Patel, A. H. (2002). Analysis of antigenicity and topology of E2 glycoprotein present on recombinant hepatitis C virus-like particles. *J Virol* **76**, 7672–7682.

Cordin, O., Banroques, J., Tanner, N. K. & Linder, P. (2006). The DEAD-box protein family of RNA helicases. *Gene* **367**, 17–37.

Deckert, J., Hartmuth, K., Boehringer, D., Behzadnia, N., Will, C. L., Kastner, B., Stark, H., Urlaub, H. & Luhrmann, R. (2006). Protein composition and electron microscopy structure of affinity-purified human spliceosomal B complexes isolated under physiological conditions. *Mol Cell Biol* **26**, 5528–5543.

de Veer, M. J., Holko, M., Frevel, M., Walker, E., Der, S., Paranjape, J. M., Silverman, R. H. & Williams, B. R. (2001). Functional classification of interferon-stimulated genes identified using microarrays. *J Leukoc Biol* **69**, 912–920.

Franca, R., Belfiore, A., Spadari, S. & Maga, G. (2007). Human DEAD-box ATPase DDX3 shows a relaxed nucleoside substrate specificity. *Proteins* **67**, 1128–1137.

Fujimoto, Y., Itabe, H., Sakai, J., Makita, M., Noda, J., Mori, M., Higashi, Y., Kojima, S. & Takano, T. (2004). Identification of major proteins in the lipid droplet-enriched fraction isolated from the human hepatocyte cell line HuH7. *Biochim Biophys Acta* **1644**, 47–59.

Gururajan, R., Perry-O'Keefe, H., Melton, D. A. & Weeks, D. L. (1991). The *Xenopus* localized messenger RNA An3 may encode an ATP-dependent RNA helicase. *Nature* **349**, 717–719.

Hope, R. G. & McLauchlan, J. (2000). Sequence motifs required for lipid droplet association and protein stability are unique to the hepatitis C virus core protein. *J Gen Virol* **81**, 1913–1925.

Huang, J. S., Chao, C. C., Su, T. L., Yeh, S. H., Chen, D. S., Chen, C. T., Chen, P. J. & Jou, Y. S. (2004). Diverse cellular transformation capability of overexpressed genes in human hepatocellular carcinoma. *Biochem Biophys Res Commun* **315**, 950–958.

Ikeda, M., Yi, M., Li, K. & Lemon, S. M. (2002). Selectable subgenomic and genome-length dicistronic RNAs derived from an infectious molecular clone of the HCV-N strain of hepatitis C virus replicate efficiently in cultured Huh7 cells. *J Virol* **76**, 2997–3006.

Jamieson, D. J. & Beggs, J. D. (1991). A suppressor of yeast spp81/ded1 mutations encodes a very similar putative ATP-dependent RNA helicase. *Mol Microbiol* **5**, 805–812.

Kanai, Y., Dohmae, N. & Hirokawa, N. (2004). Kinesin transports RNA: isolation and characterization of an RNA-transporting granule. *Neuron* **43**, 513–525.

Krishnan, V. & Zeichner, S. L. (2004). Alterations in the expression of DEAD-box and other RNA binding proteins during HIV-1 replication. *Retrovirology* **1**, 42.

Leroy, P., Alzari, P., Sassoon, D., Wolgemuth, D. & Fellous, M. (1989). The protein encoded by a murine male germ cell-specific transcript is a putative ATP-dependent RNA helicase. *Cell* **57**, 549–559.

Lindenbach, B. D., Evans, M. J., Syder, A. J., Wolk, B., Tellinghuisen, T. L., Liu, C. C., Maruyama, T., Hynes, R. O., Burton, D. R. & other authors (2005). Complete replication of hepatitis C virus in cell culture. *Science* **309**, 623–626.

Lohmann, V., Korner, F., Koch, J., Herian, U., Theilmann, L. & Bartenschlager, R. (1999). Replication of subgenomic hepatitis C virus RNAs in a hepatoma cell line. *Science* **285**, 110–113.

Mamiya, N. & Worman, H. J. (1999). Hepatitis C virus core protein binds to a DEAD box RNA helicase. *J Biol Chem* **274**, 15751–15756.

McLauchlan, J. (2000). Properties of the hepatitis C virus core protein: a structural protein that modulates cellular processes. *J Viral Hepat* **7**, 2–14.

Miyanari, Y., Atsuzawa, K., Usuda, N., Watashi, K., Hishiki, T., Zayas, M., Bartenschlager, R., Wakita, T., Hijikata, M. & Shimotohno, K. (2007). The lipid droplet is an important organelle for hepatitis C virus production. *Nat Cell Biol* **9**, 1089–1097.

Moradpour, D., Wakita, T., Tokushige, K., Carlson, R. I., Krawczynski, K. & Wands, J. R. (1996). Characterization of three novel monoclonal antibodies against hepatitis C virus core protein. *J Med Virol* **48**, 234–241.

Moradpour, D., Penin, F. & Rice, C. M. (2007). Replication of hepatitis C virus. *Nat Rev Microbiol* **5**, 453–463.

Nakabayashi, H., Taketa, K., Miyano, K., Yamane, T. & Sato, J. (1982). Growth of human hepatoma cells lines with differentiated functions in chemically defined medium. *Cancer Res* **42**, 3858–3863.

Noueiry, A. O., Chen, J. & Ahlquist, P. (2000). A mutant allele of essential, general translation initiation factor DED1 selectively inhibits translation of a viral mRNA. *Proc Natl Acad Sci U S A* **97**, 12985–12990.

Owsianka, A. M. & Patel, A. H. (1999). Hepatitis C virus core protein interacts with a human DEAD box protein DDX3. *Virology* **257**, 330–340.

Pawlotsky, J. M. (2003). Hepatitis C virus genetic variability: pathogenic and clinical implications. *Clin Liver Dis* **7**, 45–66.

Pritchard, L., Corne, D., Kell, D., Rowland, J. & Winson, M. (2005). A general model of error-prone PCR. *J Theor Biol* **234**, 497–509.

Randall, G., Panis, M., Cooper, J. D., Tellinghuisen, T. L., Sukhodolets, K. E., Pfeffer, S., Landthaler, M., Landgraf, P., Kan, S. & other authors (2007). Cellular cofactors affecting hepatitis C virus infection and replication. *Proc Natl Acad Sci U S A* **104**, 12884–12889.

Ray, R. B. & Ray, R. (2001). Hepatitis C virus core protein: intriguing properties and functional relevance. *FEMS Microbiol Lett* **202**, 149–156.

Rocak, S. & Linder, P. (2004). DEAD-box proteins: the driving forces behind RNA metabolism. *Nat Rev Mol Cell Biol* **5**, 232–241.

Roingeard, P. & Hourioux, C. (2008). Hepatitis C virus core protein, lipid droplets and steatosis. *J Viral Hepat* **15**, 157–164.

Rosner, A. & Rinkevich, B. (2007). The DDX3 subfamily of the DEAD box helicases: divergent roles as unveiled by studying different organisms and in vitro assays. *Curr Med Chem* **14**, 2517–2525.

Saban, M. R., Hellmich, H. L., Turner, M., Nguyen, N. B., Vadigepalli, R., Dyer, D. W., Hurst, R. E., Centola, M. & Saban, R. (2006). The inflammatory and normal transcriptome of mouse bladder detrusor and mucosa. *BMC Physiol* **6**, 1.

Sato, S., Fukasawa, M., Yamakawa, Y., Natsume, T., Suzuki, T., Shoji, I., Aizaki, H., Miyamura, T. & Nishijima, M. (2006). Proteomic profiling of lipid droplet proteins in hepatoma cell lines expressing hepatitis C virus core protein. *J Biochem* **139**, 921–930.

Schroder, M., Baran, M. & Bowie, A. G. (2008). Viral targeting of DEAD box protein 3 reveals its role in TBK1/IKKε-mediated IRF activation. *EMBO J* **27**, 2147–2157.

Sekiguchi, T., Kurihara, Y. & Fukumura, J. (2007). Phosphorylation of threonine 204 of DEAD-box RNA helicase DDX3 by cyclin B/cdc2 in vitro. *Biochem Biophys Res Commun* **356**, 668–673.

Shavinskaya, A., Boulant, S., Penin, F., McLauchlan, J. & Bartenschlager, R. (2007). The lipid droplet binding domain of hepatitis C virus core protein is a major determinant for efficient virus assembly. *J Biol Chem* **282**, 37158–37169.

Shih, J. W., Tsai, T. Y., Chao, C. H. & Wu Lee, Y. H. (2008). Candidate tumor suppressor DDX3 RNA helicase specifically represses cap-dependent translation by acting as an eIF4E inhibitory protein. *Oncogene* **27**, 700–714.

Simmonds, P. (1995). Variability of hepatitis C virus. *Hepatology* **21**, 570–583.

Soulat, D., Burckstummer, T., Westermayer, S., Goncalves, A., Bauch, A., Stefanovic, A., Hantschel, O., Bennett, K. L., Decker, T. & Superti-Furga, G. (2008). The DEAD-box helicase DDX3X is a critical component of the TANK-binding kinase 1-dependent innate immune response. *EMBO J* **27**, 2135–2146.

Sun, M., Song, L., Li, Y., Zhou, T. & Jope, R. S. (2008). Identification of an antiapoptotic protein complex at death receptors. *Cell Death Differ* **15**, 1887–1900.

Targett-Adams, P., Chambers, D., Gledhill, S., Hope, R. G., Coy, J. F., Girod, A. & McLauchlan, J. (2003). Live cell analysis and targeting of the lipid droplet-binding adipocyte differentiation-related protein. *J Biol Chem* **278**, 15998–16007.

Targett-Adams, P., Boulant, S. & McLauchlan, J. (2008). Visualization of double-stranded RNA in cells supporting hepatitis C virus RNA replication. *J Virol* **82**, 2182–2195.

Wakita, T., Pietschmann, T., Kato, T., Date, T., Miyamoto, M., Zhao, Z., Murthy, K., Habermann, A., Krausslich, H. G. & other authors (2005). Production of infectious hepatitis C virus in tissue culture from a cloned viral genome. *Nat Med* **11**, 791–796.

Wang, H., Kim, S. & Ryu, W. S. (2009). DDX3 DEAD-Box RNA helicase inhibits hepatitis B virus reverse transcription by incorporation into nucleocapsids. *J Virol* **83**, 5815–5824.

Watashi, K. & Shimotohno, K. (2003). The roles of hepatitis C virus proteins in modulation of cellular functions: a novel action mechanism of the HCV core protein on gene regulation by nuclear hormone receptors. *Cancer Sci* **94**, 937–943.

Witteveldt, J., Evans, M. J., Bitzegeio, J., Koutsoudakis, G., Owsianka, A. M., Angus, A. G., Keck, Z. Y., Foung, S. K., Pietschmann, T. & other authors (2009). CD81 is dispensable for

hepatitis C virus cell-to-cell transmission in hepatoma cells. *J Gen Virol* **90**, 48–58.

Yanagi, M., Purcell, R. H., Emerson, S. U. & Bukh, J. (1997). Transcripts from a single full-length cDNA clone of hepatitis C virus are infectious when directly transfected into the liver of a chimpanzee. *Proc Natl Acad Sci U S A* **94**, 8738–8743.

Yedavalli, V. S., Neuveut, C., Chi, Y. H., Kleiman, L. & Jeang, K. T. (2004). Requirement of DDX3 DEAD box RNA helicase for HIV-1 Rev-RRE export function. *Cell* **119**, 381–392.

Yi, M., Ma, Y., Yates, J. & Lemon, S. M. (2007). Compensatory mutations in E1, p7, NS2, and NS3 enhance yields of cell culture-infectious intergenotypic chimeric hepatitis C virus. *J Virol* **81**, 629–638.

You, L. R., Chen, C. M., Yeh, T. S., Tsai, T. Y., Mai, R. T., Lin, C. H. & Lee, Y. H. (1999). Hepatitis C virus core protein interacts with cellular putative RNA helicase. *J Virol* **73**, 2841–2853.

Zhou, Z., Licklider, L. J., Gygi, S. P. & Reed, R. (2002). Comprehensive proteomic analysis of the human spliceosome. *Nature* **419**, 182–185.